International Journal of Engineering & Technology, 7 (4) (2018) 3726-3730

International Journal of Engineering & Technology

Website: www.sciencepubco.com/index.php/IJET
doi: 10.14419/ijet.v7i4.11939
Research paper

The effect of sintering temperature on characteristic and properties of hydroxyapatite extracted from fish scale bio-waste

Maslinda Alias [1], Sofiah Hamzah [1] *, Jasnizat Saidin [2]

[1] School of Ocean Engineering, University Malaysia Terengganu, 21030, Kuala Terengganu
[2] School of Environmental and Marine Science, University Malaysia Terengganu, Malaysia
**Corresponding author E-mail: sofiah@umt.edu.my*

Abstract

This present study focused on the extraction of HAp from fish scale waste using alkaline heat treatment sintered at different sintering tem-perature (high range) between 300° C to 1000°C. White powder hydroxyapatite was characterized in term of morphology, surface chemistry and crystallinity structure using Scanning Electron Microscopy, Fourier transform infrared spectroscopy (FTIR) and X-ray Diffraction (XRD), respectively. Analysis from XRD shows that FSHAp-1000 has good sharp peak indicating for high crystallinity of hydroxyapatite. While, the functional analysis performed FTIR determined several functional group attributed to PO42-, CO23- and OH-. As sintering tem-perature increase, the broad peak of PO42- becomes narrower. The intensity of CO32- is observed decreased at higher calcination temperature since they are release as volatile gases. Meanwhile, adsorbed water become narrower under treatment of water. The morphology of FSHAp changed upon treatment of heat especially at high temperature. As sintering temperature increase, the particle size of FSHAp becomes fines and a regular shape of FSHAp was found agglomerated.

Keywords: *Hydroxyapatite; Ceramics: Sintering; Crystallinity; Calcination*

1. Introduction

Each year, 18-30 million of tons of fish waste is discarded which is equal to 50% of total mass of fish processing industry in the world [1]. In India, bio waste and byproduct of fish are being dumped in coastal region cause a degradation of waste produce foul smell and pollution nearby water bodies [2]. According to Scalera, et al. [3] chemical analysis shows fish scale is rich with calcium in the form of carbonate and oxide due to physiological response of fish to osmolality and ionic inequality in physiological environment. Hydroxyapatite, HAp Ca10 (PO4)6(OH) 2] is inorganic constituent which similar to human bone and teeth [4]. Arising as powerful sources of bio-ceramics used in medicinal application for bone surgery, hydroxyapatite can be found abundant from natural resources, fish scale and bone [1].Recently, great attention has been given to hydroxyapatite especially in application of catalysis, fertilizers, and pharmaceutical and protein chromatography. Hydroxyapatite also has unique property to adsorb protein. As mentioned in previous report, proteins are spontaneously adsorbed onto hydroxyapatite surface while cellular attachment, proliferation and migration occur [5]. According to Jungbauer et al.[6] separation of protein and DNA has been done by using hydroxyapatite in chromatography concept. The fact that hydroxyapatite is stable, vastly superior in terms of flow rate and reproducibility over many cycles of use has gain attention for protein separation and provide a good support for enzymes. HAp is inorganic and water soluble mineral grouping in family of calcium phosphate [7]. Generally, there are two ways of synthesizing hydroxyapatite either through chemical precipitation or naturally extracted from natural resources. Synthetic hydroxyapatite involves chemical precipitation and wet method [8].Hydroxyapatite produced from natural resources are better in their metabolic activity and more dynamic response to the environment compared to the synthetic process since synthetic hydroxyapatite need an additional chemical to the process [9]

Sintering hydroxyapatite in high temperature is needed to produce a pressed form of hydroxyapatite. Previous report made by Canillas et al.[10] sintering of hydroxyapatite connect the grains and close the space resulting in larger particles. Conventionally dense and compacted ceramics are prepared under several factor of pressure, temperature, and holding time at sintering temperature. Process involve with three stages in which hydroxyapatite is compacted, hydroxyapatite is heated to its melting point, and "neck" is begin to form. While hydroxyapatite is heated, the number of bond grows and surface area is decrease. In final process, hydroxyapatite are fully bonded together leaving small diameter of pores [11] .This present study focused on the extraction of HAp from fish scale waste using alkaline heat treatment and at different sintering temperature (high range) between 300° C to 1000° C. The extracted HAp were characterized in term of morphology, surface chemistry and crystalline structure. This study has significant contribution to application of hydroxyapatite in industry such as bone grafting and bone implant since sintering hydroxyapatite at high temperature will produce high crystalline structure of FSHAp and produce pure FSHAp without trace of impurities.

2. Material and method

2.1. Extraction of hydroxyapatite from fish scale waste

Copyright © 2018 Maslinda Alias et. al. This is an open access article distributed under the Creative Commons Attribution License, which permits unrestricted use, distribution, and reproduction in any medium, provided the original work is properly cited.

Fish scale waste collected from a local market in Kuala Terengganu undergo some process in order to remove any impurities, blood, and salts. The fish scales then dried in the laboratory for overnight. Dried fish scales undertake deproteinized process using 0.1M of HCL for external washing and distilled water needed to rinse the fish scale. The clean fish scale was boiled at 70ºC for 5 to 7 hours heated in stirring mode. Next, the boiled fish scale was further treated using 50% NaOH in order to extract hydroxyapatite. An obtained white precipitate was filtered and clean several time using deionized water until the washing solution is neutral and dried at 60ºC overnight. The sample of hydroxyapatite was sintered at a different temperature range from 300ºC to 1000ºC at heating rate 5ºC/min 1 hours and cooled slowly to room temperature [12].

2.2. Characterization of hydroxyapatite

All sample of hydroxyapatite was characterized using X-ray Diffraction (XRD) using Shimadzu model XRD-6000 equipped with Cu-K (k=1.5406). The FSHAp extracted was prepared by compressing in the cassette sample holder. X-ray Diffraction is carried out to determine a compositional phase of samples before and after sintering. The radiation dose applied is 18kW Cu radiation with 30 to 40Kv and 40mA intensity. Data analyzed by this instrument were collected in the 2θ range from 3 to 80.0º with scan step 0.02º [13] and [14].

The morphology of sample was studied by field emission scanning electron microscopy (FE-SEM), HITACHI S26000N-type microscope in Institute of Oceanography, University Malaysia Terengganu operated at 10 kV. Sample powder of FSHAp was first prepared by putting on the stub and coated with gold by sputter coating machine, JFC 1600 before viewed under the microscope [15]. This technique used to prevent the sample from burnt and damage due to an electron beam.

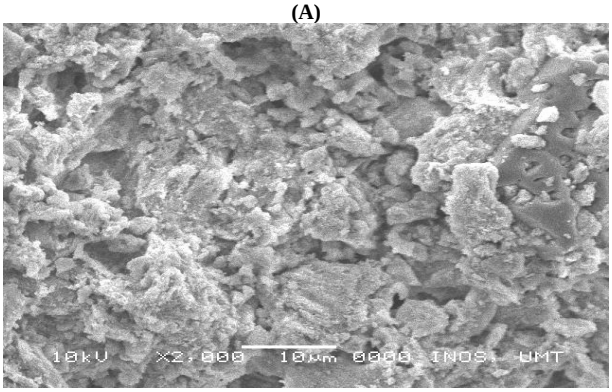
Fourier transform infrared spectroscopy (FTIR) characterization method, performed using Perkin Elmer Spectrum One with resolution 4 cm-1 in the frequency range of 4000-400 cm-1 [16]. The sample of FSHAp was prepared by the potassium bromide (KBr) pellet method. FT-IR was used to investigate the functional group of commercial and FHSAp with different calcination temperature.

3. Result and discussion

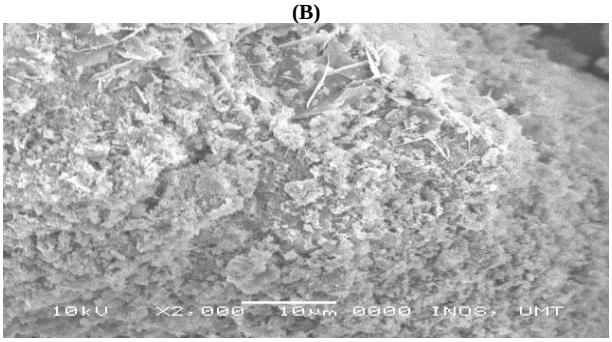
3.1. Morphology and structure of hydroxyapatite

All SEM Images of FSHAp display in the Figure 1 have different size when sintered at different temperature which similar to report made by Morbarsherpour et al. [17] mention size and shape of crystal of each sample of FSHAp vary when sintered at different temperature. In this research, FSHAp were sintered at range temperature 300ºC to 1000ºC. The result shows crystal size of FSHAp increase as sintering temperature increase. This finding is supported by Figueiredo et al. [18]. According to Pham et al. [19] sintering hydroxyapatite at high-temperature cause molecule of FSHAp move faster and colloid with each other. As temperature increase, a surface area of FSHAp also increases which creates enough strong a Van der Waals interaction to produce an agglomerate particle of FSHAp. FSHAp treated at 300ºC exhibit a needle-like a shape which similar to a report made by Zanotto et al. [20] which mention hydroxyapatite form a set of needle-like a shape with a low surface area. For FHSAp-500 in figure 1(b), the size of the hydroxyapatite decrease and more agglomerate compared to FSHAp-300. The Figure 1(c) shows SEM image from the sample of hydroxyapatite sintered at 700ºC with tiny particles of hydroxyapatite start to coalesce and form agglomeration. According to Teh et al.,[21] the powders particles of hydroxyapatite sintered at high temperature tend to fuse together and form larger agglomerates. FSHAp-900 in Figure 1(d) depicts soft agglomerates behavior when sintered at 900ºC and no formation of flakes like a shape detected as agglomeration start to take place. Present work has a similar finding to past work reported by Venkatesan & Kim [22] where microstructure of hydroxyapatite found with the increase in temperature at 900ºC. Alif et al. [23] described hydroxyapatite sintered at 900ºC were agglomerated with variable size pore evenly distributed. HAp-1000 become more agglomerated and has a homogenous distribution compared to hydroxyapatite sintered at a lower temperature. This finding also discussed in an earlier report made by Adak & Purohit [24], grain of hydroxyapatite are rounded and coalescent is reduced and preceding mechanism of particle arrangement was identified which respected to higher values of HAp.

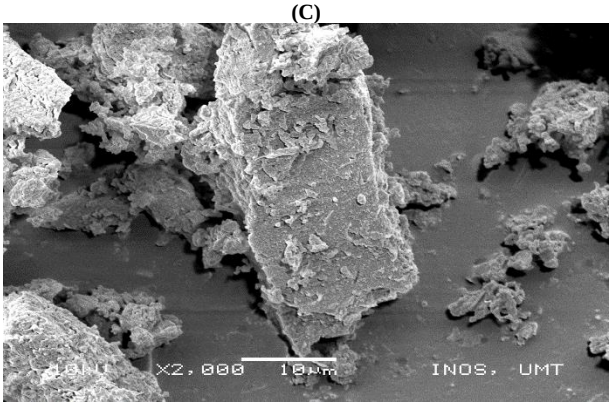
(A)



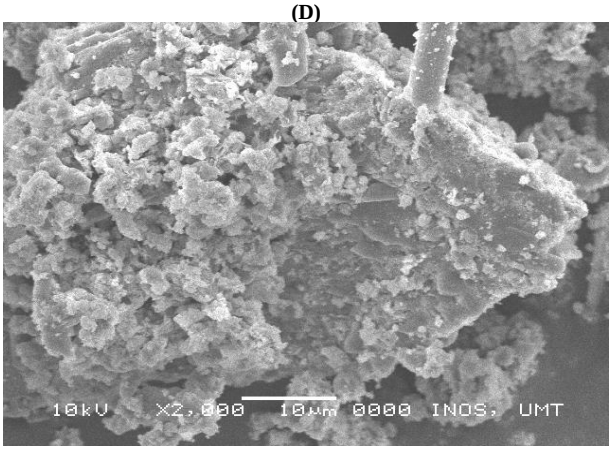
(B)



(C)



(D)



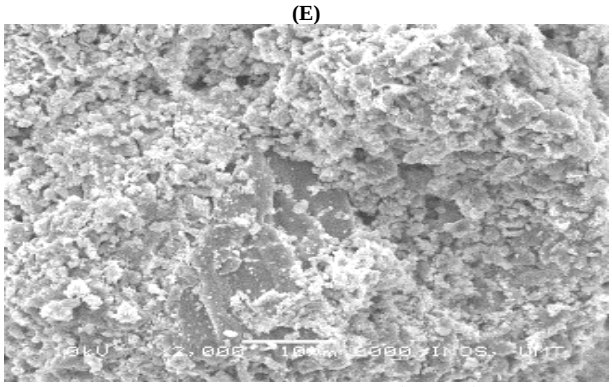


Fig. 1: Fig 1: SEM Images with Several Magnification for Sintered Fshap at (A) 300ºc, (B) 500ºc (C) 900ºc and (D) 1000ºc.

3.2. FTIR analysis

Figure 2 shows a vibrational band of the different sample of FSHAp. The FTIR has detected several significant functional group corresponding to synthesized FSHAp. The peak was attributed to a phosphate group, hydroxyl group, and carbonate group. Figure 2(b) display a spectrum exhibited by FSHAp-300 shows small band indicates for O-H stretching bond at wavelength 3988.79 cm^{-1}. Followed by adsorptive water which is relatively wide denoted by wavelength from 3600 to 2600. A vibrational peak could be assigned to functional group CO_3^{2-} displayed at wavelength 2233 cm-1. The intensity of CO_3^{2-} probably decreased at higher calcination temperature since they are released as volatile gases [25]. There are three peaks distributed attributed to PO_4^{2-}. The first peak denotes found at wavelength 1485 $cm^{-1,}$ 1031.92 cm^{-1}, and 457.13 cm^{-1}. The intensities of absorption of these band increased with an increase of calcination temperature of FSHAp powder. Increase in calcination temperature produced a narrow stretching band of adsorbed denoted by water wavelength 2357.01cm-1. The results were in agreement with Ahmed et al. [26] which reported adsorbed water becomes narrower under the treatment of heat. Another significant peak attributed to CO_3^{2-} also found at wavelength 1409.96 cm^{-1} and 1186.22 cm^{-1}. A bending mode band observed corresponding to PO_4^{2-} at wavelength 1024 cm^{-1}, 746.45 cm^{-1} and 578.64 cm^{-1}. FSHAp-500 spectrum in Fig.2 (c) shows vibrational band within wave number 3550 cm^{-}3350 cm^{-1} assigned to OH^{-1} group in HAp which indicates the presence of water in HAp structure [27]. Another significant peak attributed to CO_3^{2-} was detected at wavelength 1409.96 cm^{-1} and 1186.22 cm^{-1}. Meanwhile, a bending mode band was observed corresponding to PO_4^{2-} at wavelength 1024 cm^{-1}, 746.45 cm^{-1} and 578.64 cm^{-1}. The narrow and long peak was detected from sample FSHAp-700 in Fig. 2(d). The absorption band is observed at wavelength 2360.87cm^{-1} attributed to stretching band confirmed presence of OH^{-}. An earlier report by Ahmed et al. [26], has mention presence of OH^{-} in the sample of hydroxyapatite when sintered at 900ºC. Fig.2 (e) represent FSHAp-1000 display by broad-spectrum contains functional group attribute to OH^{-} with ion stretching mode ranging from wavelength 3400 cm^{-1} which engaged in amorphous solid. Asymmetric stretching of CO_3^{2-} is observed at wavelength 1406.11 cm^{-1} while the asymmetric stretching mode belongs to PO_4^{2-} at wavelength was detected at wavelength 1012.63 cm^{-1}. The second CO_3^{2-} was found present with out of plane bending mode at wavelength 873.33 cm^{-1}. The FTIR also shows the last functional group indicating for HAp presence which is PO_4^{2-} with asymmetric bending vibration at 559.36 cm^{-1}. FSHAp-1000 shows a sharp peak of phosphate group indicating the crystallinity of hydroxyapatite increase when calcination temperature increase. Sukaimi et al. [28] have mentioned, a complete synthesis of HAp occur when base skeletal moieties of phosphate and calcium are present.

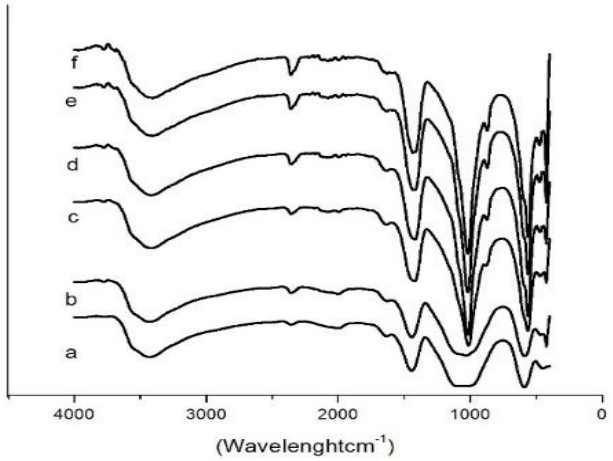


Fig. 2: A) Commercial Hap; B) Fshap-300; C) Fshap-500, D) Fshap-700; E) Fshap-900 and F) Fshap-1000.

3.3. XRD analysis

Figure 3 demonstrated the XRD pattern of hydroxyapatite isolated from fish scale waste which calcined at temperature range 300ºC to1000ºC. The XRD peaks of all five diffraction patterns are compared with commercial hydroxyapatite As shown in Figure 3, the XRD spectra with different diffraction peak of HAp confirmed the crystallinity and phase purity of hydroxyapatite obtained. Diffraction peak in Figure 3 shows that the crystal size increased with increasing calcination temperature. FSHAp samples treated at 300ºC showed a broad peak appeared at 2θ = 26.38º, 32.5º. The finding is in agreement with Sanosh et al. [29] which were reported has low intensity and a wide peak indicating poor crystallinity. According to Figueiredo et al. [18] the poor crystallinity occurs when carbonate is substituted as a mineral.

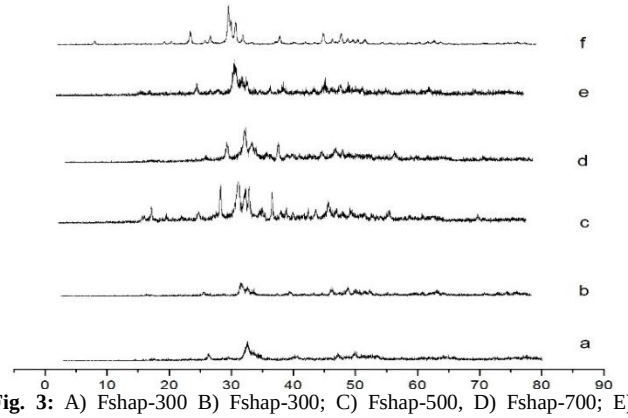


Fig. 3: A) Fshap-300 B) Fshap-300; C) Fshap-500, D) Fshap-700; E) Fshap-900 and F) Commercial Hap.

Meanwhile, FSHAp-500 in Figure 3(c) display a characteristic peak at 2θ= 26.22º and 34.92º indicates for low crystallinity. There was slightly change in Figure 3(d) to width and height of peak at 2θ= 32.36º when sintering temperature was increased up to 700ºC. This finding is supported by Mustafa et al. [9], which reported increasing in sintering temperature had increased the peak intensity of hydroxyapatite and decrease the width of the peak as well. Others stated that a lattice parameter of HAp will be increased with an increasing temperature and the changes in crystal size [27]. The high intensity of apatite is probably due to a removal of organic traces and substances from the powder of hydroxyapatite [23]. For FSHAp-900ºC, the strong characteristic peak of HAp was observed at position 2θ = 33.33º. When sintered at high temperature, apatite peak of hydroxyapatite become sharper due to crystal growth [23]. FSHAp-1000 in Figure 3(e) exhibit strong intensity and a sharp peak at 2θ=32.32º. According to Mondal et al. [30], hydroxyapatite sintered at a temperature between 800ºC to 1200ºC has distinct and narrower peak which suggest an increase in the degree of crystallinity. Furthermore, FSHAp-1000

shows a small shift in position at 2θ compared to commercial hydroxyapatite. According to Venkatesan & Kim [23], a small shifting of diffraction is due to dehydroxylation of HAp phase. Despite having high intensity of apatite peak, FSHAp-1000 shows no presence of β-tricalcium phosphate, β-TCP, and TCP which indicate no impurities presence in synthesized powder. According to Abdal-hay et al. [31] the impurities present when temperature supply to sample of hydroxyapatite is not enough to overcome the activation energy and shortage of annealing time as well while TCP is formed when hydroxyapatite sintered at the temperature more than 1000ºC which lead to dissociation of HAp [21]. Since FSHAp-1000 has the sharp peak and strong intensity without the presence of other calcium phosphates, it proves that sintering hydroxyapatite at 1000ºC is sufficed to produce high crystallinity of hydroxyapatite.

4. Conclusion

In this present study, hydroxyapatite was successfully isolated from fish scale bio waste via alkaline heat treatment. Characterization of FSHAp prove that at high sintering temperature, FSHAp exhibit excellent crystallinity when analysed by XRD attributed to high crystallinity while express sharp peak associated with PO_4^{2-} while intensity of CO_3^{2-} decrease at higher temperature since the functional group release as volatile gases and adsorption water band becomes narrower. In addition, FSHAp-1000 was found agglomerated and has homogenous distribution compared to hydroxyapatite sintered at a low temperature.

Acknowledgement

The authors wish to express high gratitude to the Ministry of Higher Education Malaysia for the funding of this research (FRGS 59354). Thank you also for the contribution and support from the School of Ocean Engineering, Central Lab and Institute of Biotechnology Marine, Universiti Malaysia Terengganu.

References

[1] N. Muhammad, Y. Gao, F.Iqbal, P.Ahmad, R.Ge, U. Nishan, Z.Ullah, Extraction of biocompatible hydroxyapatite from fish scales using novel approach of ionic liquid pretreatment, Separation and Purification Technology 161 (2016), 129–135. https://doi.org/10.1016/j.seppur.2016.01.047.

[2] F.Scalera, F. Gervaso, K.P. Sanosh, A. Sannino, A.Licciulli, Influence of the calcination temperature on morphological and mechanical properties of highly porous hydroxyapatite scaffolds, *Ceramics International* 39(5) (2013) 4839–4846. https://doi.org/10.1016/j.ceramint.2012.11.076.

[3] N.N. Panda, K. Pramanik & L. B. Sukla, Extraction and characterization of biocompatible hydroxyapatite from fresh water fish scales for tissue engineering scaffold, Bioprocess and Biosystems Engineering 37(3) (2014) 433–440. https://doi.org/10.1007/s00449-013-1009-0.

[4] A. Costescu, L. Pasuk, F. Ungureanu, A. Dinischiotu, F. Huneau, S. Galaup, C.Ftir, Physico-Chemical Properties of Nano-Sized Hexagonal Hydroxyapatite Powder Synthesized By Sol-Gel, Digest Journal of Nanomaterials and Biostructures 5 (4) (2010) 989–1000.

[5] S. Zhao, Z. Wang, J. Wang, S. Wang, Poly(ether sulfone)/polyaniline nanocomposite membranes: Effect of nanofiber size on membrane morphology and properties, Industrial and Engineering Chemistry Research 53 (28) (2014) 11468–11477. https://doi.org/10.1021/ie501235t.

[6] A. Jungbauer, R. K. Deinhofer, P . Luo, Performance and characterization of a nanophased porous hydroxyapatite for protein chromatography, Biotechnology and Bioengineering 87 (3) (2014) 364–375. https://doi.org/10.1002/bit.20121.

[7] T. Jesionowski, J. Zdarta, B. Krajewska, Enzyme immobilization by adsorption: A review, Adsorption 20 (5–6) (2014) 801–821. https://doi.org/10.1007/s10450-014-9623-y.

[8] M. Ansari, S. M. Naghib, F. Moztarzadeh, A. Salati, Synthesis and characterization of hydrxyapatite calcium hydroxide for dental composites. Ceramics 67 (5) (2015) 123–126 .

[9] N. Mustafa, M. H. Ibrahim, R. Asmawi, M. A. Amin, Hydroxyapatite Extracted from Waste Fish Bones and Scales via Calcination Method, Applied Mechanics and Materials 773–774 (2015) 287–290. https://doi.org/10.4028/www.scientific.net/AMM.773-774.287.

[10] M. Canillas, R. Rivero, R. García-Carrodeguas, F. Barba, M.A. Rodríguez, Processing of hydroxyapatite obtained by combustion synthesis, Boletin de La Sociedad Espanola de Ceramica Y Vidrio 56 (5) (2017) 237–242. https://doi.org/10.1016/j.bsecv.2017.05.002.

[11] M. Prakasam, M. J. Locs, J. K. Salma-Ancane, K. D. Loca, A. Largeteau, L. Berzina-Cimdina, Fabrication, properties and applications of dense hydroxyapatite: A review, Journal of Functional Biomaterials 6 (4) (2015) 1099–1140. https://doi.org/10.3390/jfb6041099.

[12] W. Khoo, F. M. Nor, H. Ardhyananta, D. Kurniawan, Preparation of Natural Hydroxyapatite from Bovine Femur Bones Using Calcination at Various Temperatures, Procedia Manufacturing 2 (2015) 196–201. https://doi.org/10.1016/j.promfg.2015.07.034.

[13] V. Kalaiselvi, R. Mathammal, P. Anitha, Sol-Gel Mediated Synthesis of Pure Hydroxyapatite at Different Temperatures and Silver Substituted Hydroxyapatite for Biomedical Applications, Journal of Biotechnology & Biomaterials 6 (4) (2017) 00-00.

[14] S. Kongsri, P. L.N. Ayuttaya, S. Yookhum, S. Techawongstein, S. Chanthai, Characterization of hydroxyapatite nanoparticles from fish scale waste and its adsorption of carotenoids, Asian Journal of Chemistry 25 (10) (2013) 5847–5850.

[15] T. Nagasaki, F. Nagata, M. Sakurai, K. Kato, Effects of pore distribution of hydroxyapatite particles on their protein adsorption behavior, Journal of Asian Ceramic Societies 5 (2) (2017) 88–93. https://doi.org/10.1016/j.jascer.2017.01.005.

[16] N. Jamarun, A. Asril, Z. Azharman, T. P. Sari, S. W. Sumatera, Effect of hydrothermal temperature on synthesize of hydroxyapatite from limestone through hydrothermal method, Research Article 7 (6) (2015) 832–837.

[17] I. Mobasherpour, M. S, Heshajin, A. Kazemzadeh, M. Zakeri, Synthesis of nanocrystalline hydroxyapatite by using precipitation method, Journal of Alloys and Compounds 430 (1-2) (2007) 330-333. https://doi.org/10.1016/j.jallcom.2006.05.018.

[18] M. Figueiredo, A. Fernando, G. Martins, J. Freitas, F. Judas, H. Figueiredo, Effect of the calcination temperature on the composition and microstructure of hydroxyapatite derived from human and animal bone, Ceramics International 36 (8) (2010) 2383–2393. https://doi.org/10.1016/j.ceramint.2010.07.016.

[19] T.T.T. Pham, T. P. Nguyen, T. N. Pham, T. P. Vu, D. L, Tran, H. Thai, T.M.T. Dinh, Impact of physical and chemical parameters on the hydroxyapatite nanopowder synthesized by chemical precipitation method, Advances in Natural Sciences: Nanoscience and Nanotechnology 4 (3) (2013) 035014.

[20] A. Zanotto, M. L Saladino, D. C. Martino, E. Caponetti, Influence of Temperature on Calcium Hydroxyapatite Nanopowders, Advances in Nanoparticles 1 (3) (2012) 21–28. https://doi.org/10.4236/anp.2012.13004.

[21] Y. C. Teh, C.Y. Tan, S. Ramesh, J. Purbolaksono, Y. M. Tan, H. Chandran, W. D. Teng, B. K.Yap, Effect of powder calcination on the sintering of hydroxyapatite, The Medical Journal of Malaysia 63 (21) (2008) 87–88.

[22] M. F. Alif, W. Aprillia, S. Arief, Peat Water Purification by Hydroxyapatite (HAp) Synthesized from Waste Pensi (bvg7*Corbicula moltkiana*) Shells, IOP Conference Series: Materials Science and Engineering 299 (1) (2018) 12002. https://doi.org/10.1088/1757-899X/299/1/012002.

[23] J. Venkatesan, S. K, Kim, Effect of temperature on isolation and characterization of hydroxyapatite from tuna (thunnus obesus) bone, Materials 3(10) (2010) 4761- 4772. https://doi.org/10.3390/ma3104761.

[24] M. D. Adak, K. M. Purohit, Synthesis of nano-crystalline hydroxyapatite from dead snail shells for biological implantation, Trends in Biomaterials and Artificial Organs 25 (3) (2011) 101–106.

[25] D. K. Pattanayak, R. Dash, R. C Prasad. B.T. Rao, T. R. Rama Mohan, Synthesis and sintered properties evaluation of calcium phosphate ceramics, Materials Science and Engineering: C 2 (74) (2007) 684–690. https://doi.org/10.1016/j.msec.2006.06.021.

[26] Y. M. Ahmed, S. M. El-Sheikh, S. I. Zaki, Changes in hydroxyapatite powder properties via heat treatment, Bulletin of Materials Science 38 (7) (2015) 1807–1819. https://doi.org/10.1007/s12034-015-1047-0.

[27] D. Malina, K. Biernat, A. Sobczak-Kupiec, Studies on sintering process of synthetic hydroxyapatite, Acta Biochimica Polonica 60 (4) (2013) 851–855.

[28] J. Sukaimi, S. Hamzah, M. S. M. Ghazali, Green Synthesis and Characterization of Hydroxyapatite From Fish Scale Biowaste, Applied Mechanics and Materials 695 (2015) 235–238.
[29] K. P. Sanosh, M. Chu, A. Balakrishnan, T. N. Kim, S-J. CHO, Preparation and characterization of nano-hydroxyapatite powder using sol – gel techniqu, Bulletin of Material Science 32 (5) (2009) 465–470. https://doi.org/10.1007/s12034-009-0069-x.
[30] A. Abdal-hay, A. Barakat, N. A. M., & L. J. Kyoo, Hydroxyapatite-doped poly (lactic acid) porous film coating for enhanced bioactivity and corrosion behavior of AZ31 Mg alloy for orthopedic applications, Ceramics International 39 (2013) 183–195. https://doi.org/10.1016/j.ceramint.2012.06.008.
[31] S. Mondal, B. Mondal, A. Dey, S. S. Mukhopadhyay, Studies on Processing and Characterization of Hydroxyapatite Biomaterials from Different Bio Wastes, Journal of Minerals and Materials Characterization and Engineering 11 (1) (2012) 55–67. https://doi.org/10.4236/jmmce.2012.111005.